Pulse Sharpening and RF Generation Using Nonlinear Transmission Lines*

L.P. Silva Neto[1], J.O. Rossi, J.J. Barroso
Associated Plasma Laboratory
National Institute for Space Research
Sao Jose dos Campos, Brazil
[1]silvaneto007@yahoo.com.br

***Abstract*— A nonlinear lumped element transmission line (NLETL) with linear inductors and using capacitors as nonlinear elements was built to operate as a high voltage pulse sharpener. NLETLS are suitable for use in fast sampling pulse generation circuits and in the formation of high-voltage solitons, among other applications. In this paper, a NLETL built with 30 sections was tested up to 500 V providing a pulse rise reduction of 700 ns for an input rise time of about 2.5 µs on a 70 ohms resistive load when using a 1.2 kV IGBT solid state switch. Comparison of experimental results with Spice simulation from equivalent NLTL circuit modeling has shown good agreement.**

Keywords— pulse compression; nonlinear capacitor; nonlinear transmission line.

I. INTRODUCTION

Nonlinear lumped element transmission lines (NLETLs) have been studied for pulse compression and high power radio frequency (RF) generation [1]-[9]. A NLETL is a ladder network comprising nonlinear capacitors and/or inductors. NLETL with nonlinear capacitor is called a nonlinear capacitive line (NLCL) and a NLETL with nonlinear inductors a nonlinear inductive line (NLIL). When using both nonlinear elements (L and C) it is known as hybrid line. Studies have shown that NLETLs reduce rise time by pulse sharpening, which can be useful in high-speed sampling and timing systems [1]. Using ceramic capacitors, Ibuka et al. [2] have built a NLTL and employed the pulse-sharpening scheme in a CO_2 laser power supply. The pulse applied on the line had 20 kV of amplitude with rise time of 500 ns, and the output pulse rise-time obtained was less than 120 ns, giving a rise time reduction of about 380 ns [2]. Pulse sharpening is based on wave propagation in a nonlinear medium. For example, assuming that a voltage pulse is injected into the NLCL input and that the capacitance decays with the applied voltage, the propagating pulse portion of higher amplitude travels faster than that of lower intensity, since the propagation phase velocity of a voltage pulse in a nonlinear LC ladder is given by:

$$v_p = \frac{1}{\sqrt{LC(V)}}, \qquad (1)$$

where L is the inductance per section and C(V) is the capacitance per section at the applied voltage V. Then v_p is expressed in units of section/ second. The reduction in rise time can be estimated as [3]:

$$\Delta T = t_{ri} - t_{ro} = \partial_1 - \partial_2 = n\left(\sqrt{LC_0} - \sqrt{LC(V_{max})}\right), \qquad (2)$$

The pulse rise time reduction in a NLELT is depicted in Fig. 1.

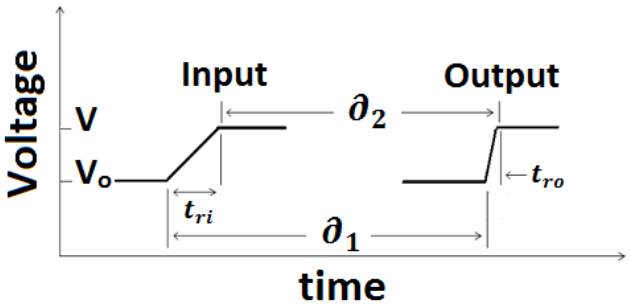

Fig. 1. Pulse compression in a NLETL

where t_{ri} is the input rise time, t_{ro} the output rise time, n is the number of sections of the line, C_0 the unbiased capacitance and $C(V_{max})$ the capacitance at the full input pulse amplitude.

Other NLETL applications include soliton wave generation in the radiofrequency (RF) range for UWB radars used in satellites and defense mobile platforms. Soliton waves from a NLCL can reach peak power of the order of hundreds of MW in the RF range. For instance, a group from Oxford University built a NLCL that produced a 175 MW peak power at a frequency of about 80 MHz [4]. On the other hand, other group from BAE Systems Company (UK) constructed a counterpart NLIL, achieving higher frequency operation (1 GHz) but with lower peak power of 20 MW [5].

In this work, we describe the implementation of a sharpening pulse generator based on high voltage nonlinear capacitive line (NLCL) using commercial-off-the-shelf (COTS) ceramic capacitors. Corresponding NLCL Spice simulation is also provided for comparison with experimental results.

II. DESCRIPTION OF THE NLCL PULSER

The NLCL schematic circuit is shown in Fig. 2. A pump input pulse generator is required to inject a rectangular pulse onto the line. The pump pulse generator consists of a storage capacitor (C1//C2) and a high voltage (HV) switch (an IGBT

*Work supported by SOARD-USAF under contract number no.FA9550-14-1-0133, CAPES and MCTI, Brazil.

transistor with holding-off capability of 1.2 kV). As shown in Fig. 2, a DC high voltage source acquired from Gamma Company charges the storage capacitors up to the nominal voltage and a low voltage pulse generator triggers the HV switch to discharge the storage capacitor for producing the pump input pulse. This input pulse travels along the line and emerges with faster rise time delayed at the output on a resistive load of 50 ohms. The high voltage diodes D5 to D10 are used to protect the HV switch against negative back swing voltage, while D4 diode for reverse current. Because of the HV circuit configuration, a pulse transformer is used to isolate the pulse trigger pulse generator from the IGBT gate.

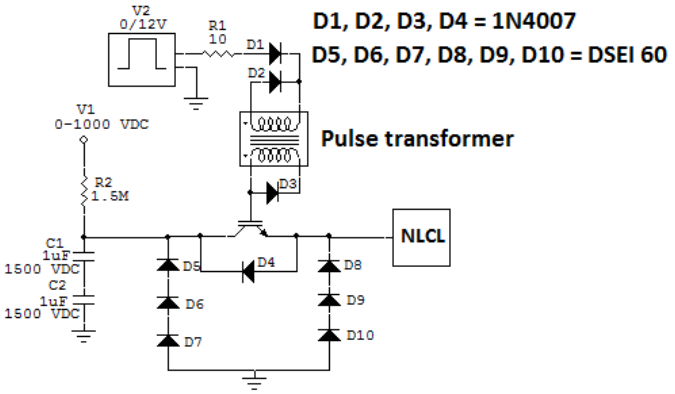

Fig. 2. Electrical circuit with IGBT switch used to drive a NLCL.

III. Experimental Results

This section is concerned with the construction and test of the high voltage pulsed system, measurement circuits, and dielectric characterization of COTS components, namely, $BaTiO_3$-based ceramic capacitors.

A. High voltage NLCL and pulse generator

A typical 0.2 kV discharge pulse from storage capacitor using IGBT switch into a 2 kΩ load without the NLCL is given in Fig. 3. The discharge pulse produced has a waveform that is almost rectangular in shape in the most part, not considering the long fall time.

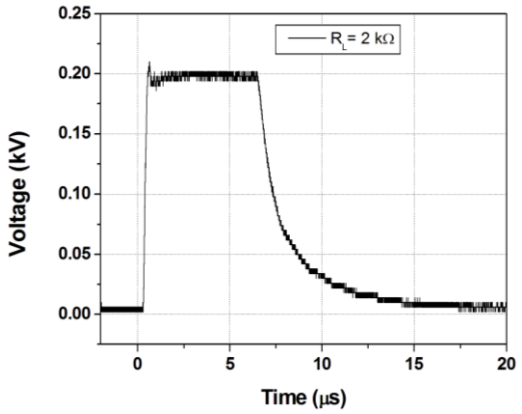

Fig. 3. Output pulse obtained from IGBT switch connected to a 2 kΩ resistive load.

The NLCL consists of 30 sections, where each section contains a single L connected to a single C as shown in Fig. 4. The linear inductance in each section has a value of 3.3 μH with unbiased nonlinear capacitance of 1.0 nF. Resistors R_L = 0.16 Ω and R_C = 2.0 Ω account for losses in the inductors and capacitors, respectively, as justified in [6].

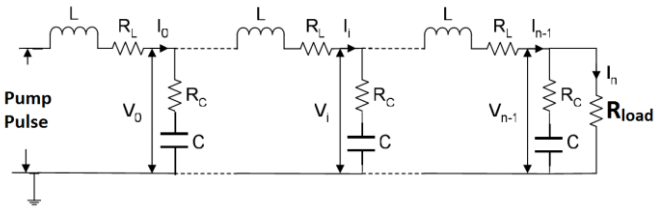

Fig. 4. NLCL using ceramic capacitor and linear inductor with 30 section.

B. Nonlinear capacitance characteristics

The electric permittivity and capacitance as function of the applied voltage measured under DC (static) condition for the 1.0 nF ceramic capacitor is shown in Fig. 5. For this measurement, the capacitor under test is charged via a DC power supply, where a C-meter in series with a linear capacitor of higher capacitance and the device measures the desired component capacitance [7]. The dielectric permittivity ε_r of the capacitor under test is calculated as:

$$\varepsilon_r = \frac{Cd}{\varepsilon_0 A}, \qquad (3)$$

where C is the capacitance measured, d the dielectric thickness, A the dielectric area and ε_0 the free-space vacuum permittivity. Fig. 5 shows the measured capacitance as a function of the applied voltage for capacitor C#1 with 1 nF of capacitance. It is seen that the capacitance decreases by 50 % ~~of~~ from its original value near the capacitor nominal voltage (2.0 kV), illustrating the behavior of a nonlinear capacitor.

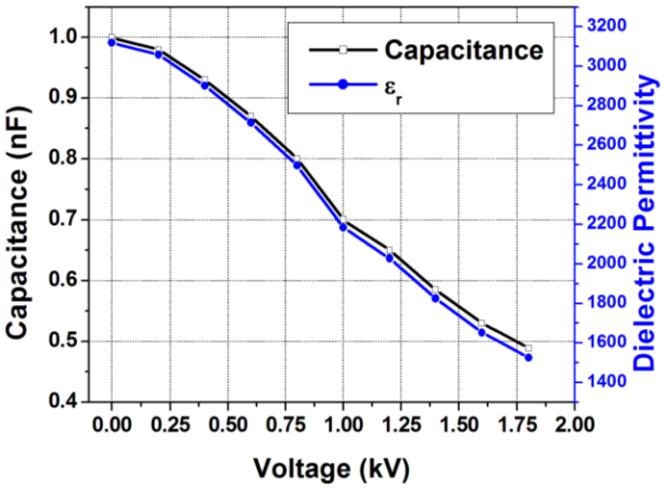

Fig. 5. Variation of the capacitance and dielectric permittivity with applied voltage.

Fig. 6 shows the nonlinearity behavior as function of applied voltage for capacitor C#2 with 10 nF of capacitance. It is seen that the capacitance decreases by 93 % of its original value near the capacitor nominal voltage (2.0 kV), illustrating the strong nonlinear behavior.

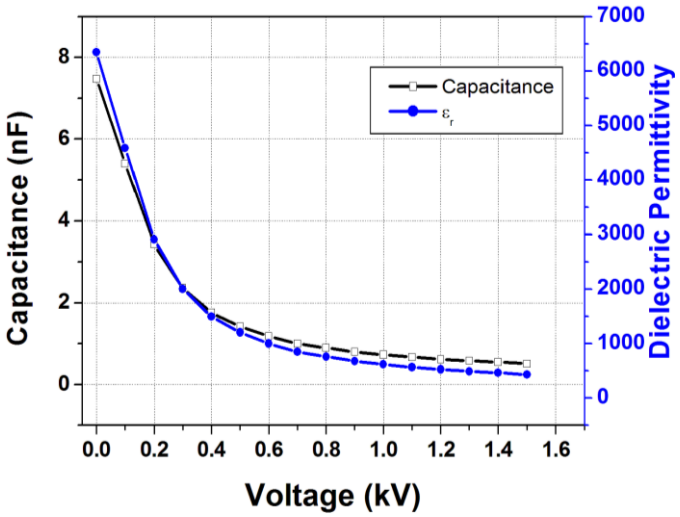

Fig. 6. Variation of the capacitance and dielectric permittivity with applied voltage.

Fig. 7 shows the NLCL PCB (printed circuit board) tested with 30 sections. First, the IGBT switch was used to discharge the storage capacitor onto the NLCL. In this case, the IGBT nominal voltage limited the pump pulse amplitude applied on the line up to 1.2 kV. The voltage source was set to 1.0 kV and a resistance of 30 ohms was placed between the line input and switch to limit the current for switch protection. Because of this, the input pulse amplitude obtained is of the order of 450 V as shown in Fig. 8 by the blue line. The input pulse rise-time is of the order of 2.5 µs and the compressed output pulse has a rise time of about 1.8 µs, giving a reduction of about 700 ns, according to (2). Also, observe in Fig. 8 that the output pulse in red line is delayed by the line propagation time (of the order 700 ns) as expected and has a slight amplitude above that of the input pulse due to the reflection caused by the load (of 70 ohms) unmatched to the impedance of the unbiased line (of about 57 ohms). This impedance value is readily calculated from

$$Z = \sqrt{\frac{L}{C(V)}}, \qquad (4)$$

with L = 3.3 µH and C(v) = 1.0 nF.

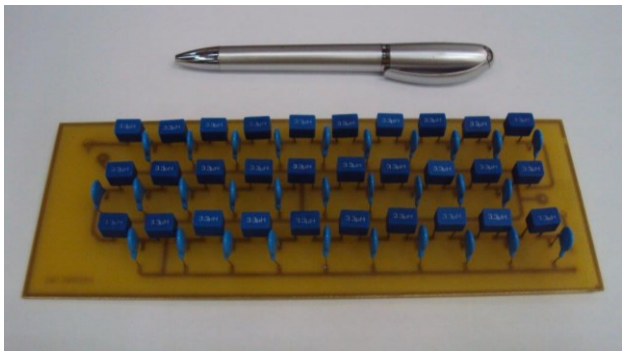

Fig. 7. NLCL assembled in the printed circuit board.

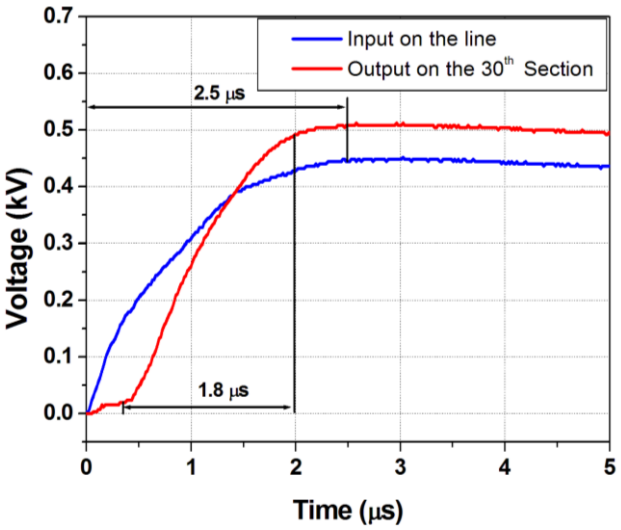

Fig. 8. Input pulse and sharpened output pulse on a load of 70 Ω using C#1 in the NLTL.

Using ceramic capacitor C#2 with strong nonlinear effect (93 % capacitance variation) in the line, soliton generation is obtained at the line output as demonstrated in Fig. 9. The rise time of input pulse is 2.0 µs (blue line) and Δt = 3.27 µs (calculated).

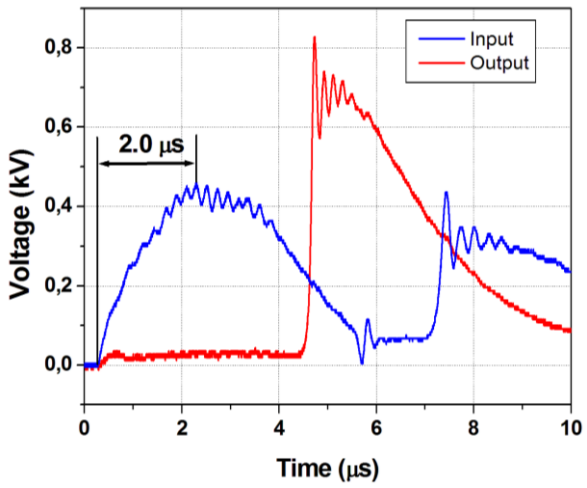

Fig. 9. Input pulse and sharpened output pulse on a load of 70 Ω.

The frequency of the soliton signal generated using C#2 is of the order of 3.2 MHz as shown by the Fourier transform spectrum in Fig. 10.

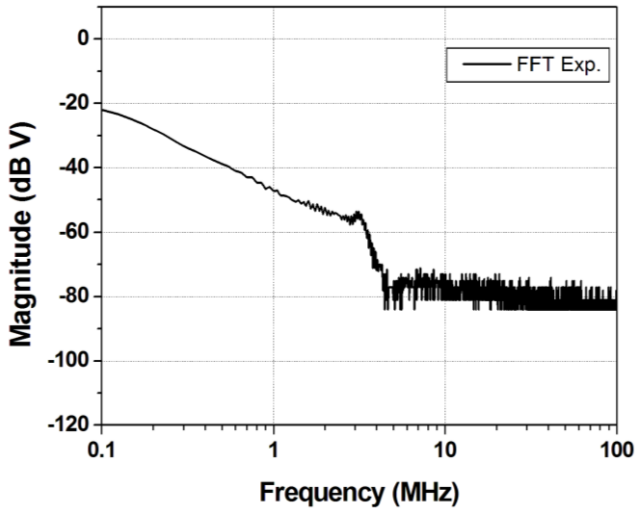

Fig.10. Frequency spectrum obtained of the periodic train of solitons.

IV. SPICE SIMULATION

To model the behavior of the high voltage sharpener a circuit model is implemented in the circuit simulator LT-Spice, which is able to model nonlinear components by using hyperbolic or exponential functions. In the case of a nonlinear capacitor, the equation below models the characteristics of a nonlinear capacitor as function of applied voltage:

$$C(V) = (C_0 - C_1).\left[1 - tanh^2\left(\frac{V}{V1}\right)\right] + C_1, \qquad (5)$$

where C(V) is the capacitance at the full pulse amplitude, C_0 is the unbiased capacitance, and C_1 and V_1 are fitting parameters. For instance, Fig. 11 shows the modeled C(V) curve obtained from (5) with C_0 = 1.0 nF, V_1 = 1200 V, C_1 = 0.38 nF compared to the experimental capacitance-voltage dependence measured under DC static condition (see also Fig. 5). As shown, a good fitting between modeling and experimental results is observed, which demonstrates the validity of the model used.

For implementing the proper nonlinear model in the LT-Spice simulator, a command for the value of the charge is required. Since nonlinear capacitance is a differential quantity, defined as C(V) = dQ/dV, the stored charge as function of the known capacitance is [8]

$$Q(V) = \int_0^V C(V')dV', \qquad (6)$$

Combining (5) and (6) we then obtain:

$$Q(V) = (C_0 - C_1).V_1.tanh\left(\frac{V}{V1}\right) + C_1V \qquad (7)$$

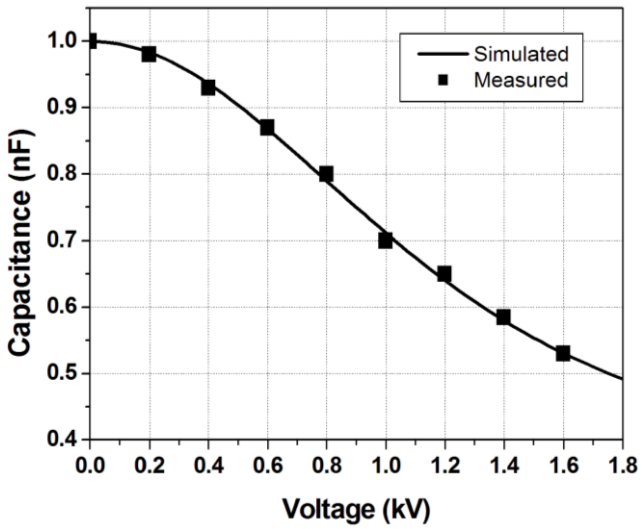

Fig. 11. Simulated and measured C-V characteristics.

Fig. 12 shows the simulation results obtained for the input and sharpened output pulses, demonstrating a good agreement with the measured waveforms in Fig. 8. The simulated output pulse shape (red line) shows a pulse rise-time reduction of the order 600 ns, giving an output rise time of about 2.2 µs. The blue line represents the input pulse with rise time of the order of 2.8 µs, which is in reasonable agreement with the measured pulse shape. In order to obtain a good fitting the line capacitor parameters were obtained from the C-V curve measured under dynamic conditions [8]. In particular, for these simulations the values used for C were C_0 = 0.5 nF and C_1 = 0.1 nF with V_1 = 650V for an ideal switch with internal inductance of 50 µH. During the capacitor discharge, as noted by Siang [8], the unbiased capacitance, saturation voltage and capacitance measured on dynamic tests (C_0, V_1 and C_1, respectively) are much lower than measured under DC static condition as shown in Fig. 5. Using these values of C_0 and C_1 into (2) one obtains a pulse rise-time reduction of the order 660 ns, very near the value obtained in the experiment.

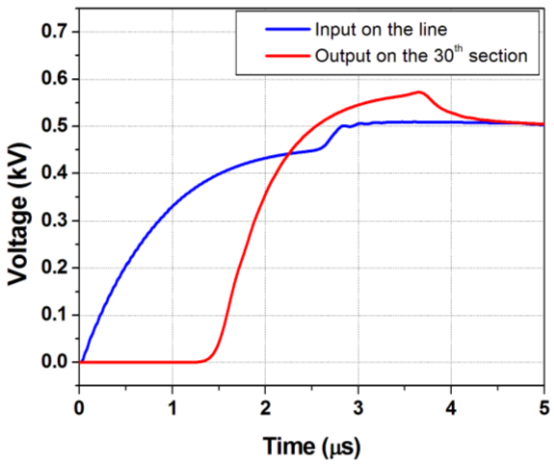

Fig. 12. Simulation result showing pulse sharpening at the NLCL output using C#1 as nonlinear capacitor.

An important experimental observation was to consider the variation of the switch parameter on LT simulation. When the switch inductance was decreased from 30 µH to 1 µH, a faster input pulse rise time of the order of 0.35 ns (< the time reduction factor of 660 ns) was obtained according to Fig. 13. In this case, the output pulse rise-time is limited by the cutoff frequency of the lumped line, as the output front slope cannot become infinite or negative. As a result, the simulated output pulse emerges delayed at the load, and is broken into a train of solitons superimposed on its full amplitude as seen in Fig. 13. In this case, because of the weak nonlinearity of the capacitor used in the line, the amplitudes of oscillations are not high enough and they die away after only three cycles. In principle, these oscillations depending on the modulation depth and line losses could be used as RF signals in mobile defense platforms, satellite communications, radars and military applications [9]. This last simulation result is very important for the NLCL design since it demonstrates the importance of obtaining fast switching of less than several hundred of ns for soliton generation in nonlinear transmission lines. Other important aspect is that the nonlinearity factor of the nonlinear capacitor must be of the order of 10 % or less to produce oscillations of higher amplitudes for NLCLs used for operation as RF source systems as observed during simulations.

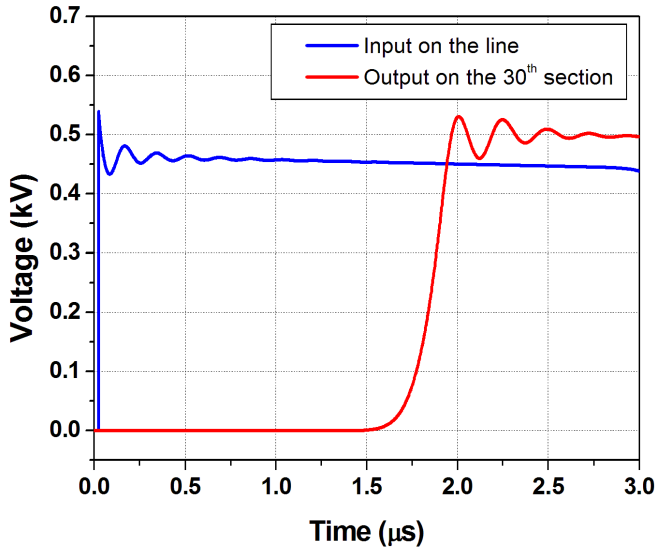

Fig. 13. Soliton generation in the NLCL using faster switching and C#1 as nonlinear capacitor.

The Fast Fourier Transform (FFT) was taken to determine the frequency of soliton oscillations, as shown in Fig. 14. In this case the frequency obtained in the output of the line is on order of 4.0 MHz with RF peak power of around 150 W.

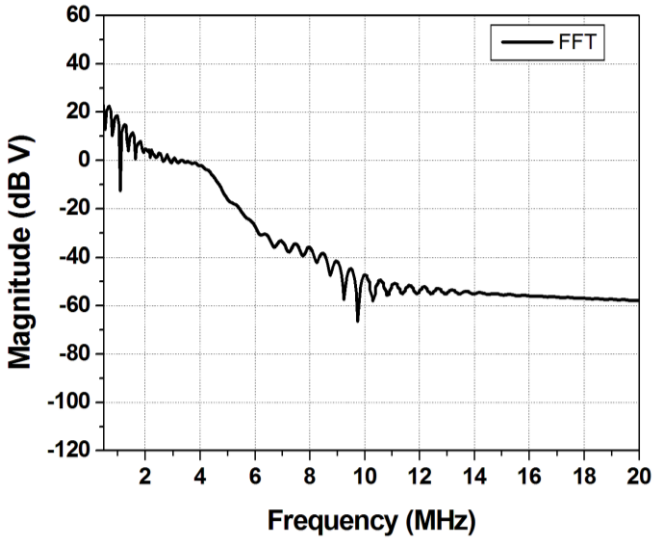

Fig. 14. Frequency spectrum of the periodic train of solitons.

V. CONCLUSIONS

Pulse sharpening was achieved using a ladder-type NLCL. Using C#1 as nonlinear capacitor in the NLCL, the nonlinearity was not so high to produce soliton generation for an input rise time in the microsecond range. The pulse rise reduction obtained was of order of 700 ns for the sharpened output pulse, in good agreement with simulation results. But using C#2 as nonlinear ceramic capacitor soliton was generated with a frequency on order of 4 MHz in the output of the NLCL due a strong nonlinearity of 93 %. A final important conclusion is that nonlinear capacitor parameters such unbiased capacitance, voltage and capacitance at saturation are much lower when submitted to dynamic conditions during the application of the input pulse as demonstrated by the simulation and experimental results from a high voltage sharpener in this paper. Besides, through simulation using a low inductance switch for producing faster rise times, soliton generation was demonstrated even with capacitors of weak nonlinearity used in the NLCL tested. Finally, the more important aspect confirmed through simulations is that nonlinearity factor (< 10 %) is an important issue for producing soliton RF combined with a faster input rise time in the range of several hundred of ns.

REFERENCES

[1] E. Afshari and A. Hajimiri, “Non-linear transmission lines for pulse shaping in silicon,” in Proc. IEEE Custom Integrated Circuits Conf., San Jose, CA, USA, 2003, pp. 91-94.

[2] S. Ibuka, K. Abe, T. Miyazawa, A. Ishii, and S. Ishii, “Fast high-voltage pulse generator with nonlinear transmission line for high repetition rate operation,” IEEE Trans. on Plasma Science, vol 25, n. 2, pp. 266-271, 1997.

[3] F.S. Yamasaki, J.O. Rossi, J.J. Barroso, “RF generation using nonlinear transmission lines for aerospace applications,” in Proc. SBMO/IEEE MTT-S IMOC, Rio de Janeiro, Brazil, Aug. 2013, pp. 1–5.

[4] J.D.C. Darling and P.W.Smith, “High power pulse burst generation by soliton type oscillation on nonlinear lumped element transmission lines,”

IEEE 17th Int. Pulsed Power Conf., Washington, DC, USA, 2009, pp. 119-123.

[5] N. Seddon, C.R. Spikings, and J.E. Dolan, "RF pulse formation in nonlinear transmission lines," IEEE 16th Int. Pulsed Power Conf., Albuquerque, NM, USA, 2007, pp.678-681.

[6] N.S. Kuek, A.C. Liew, E. Schamiloglu, and J.O. Rossi, "Circuit modeling of nonlinear lumped element transmission lines including hybrid lines," IEEE Trans. Plasma Science, vol. 40, n. 10, pp. 2523-2534, 2012.

[7] L.P. Silva Neto, J.O. Rossi, J.J. Barroso, A.R. Silva Jr., P.J. Castro, P.A.G. Dias, "Characterization of ceramic dielectrics for sub-GHz applications in nonlinear transmission lines," in Proc. SBMO/IEEE MTT-S IMOC, Rio de Janeiro, Brazil, Aug. 2013, pp. 1–5.

[8] K. N. Siang, "Theoretical and experimental studies on nonlinear lumped element transmission lines for RF genertation," thesis (In Electrical Engineering- Electrical & Computer Eng. Dept.), National University of Singapore, July 2013.

[9] L.P. Silva Neto, J.O. Rossi, J.J. Barroso, A. R. Silva Junior, " Characterization of ceramic dielectrics for sub-GHz applications in nonlinear transmission lines," IEEE Trans. on Plasma Science, vol 42, n. 10, pp. 3274-3282, 2014.